

# RACCAM PROJECT: SPIRAL FFAG FOR PROTON THERAPY

J. Fourrier \*, E. Froidefond, J. Pasternak  
*Laboratoire de Physique Subatomique et Cosmologie (CNRS/IN2P3-UJF-INPG)*  
53, avenue des Martyrs, 38026 Grenoble Cedex, France. \*fourrier@lpsc.in2p3.fr

B. Autin  
*CERN, Geneva, Switzerland*

F. Méot  
*LPSC (CNRS/IN2P3-UJF-INPG), Grenoble, France and CEA DAPNIA, Saclay, France*

D. Neuvéglise, T. Planche  
*SIGMAPHI, Vannes, France*

## Abstract

High repetition rate of the FFAG accelerator and compactness of spiral type designs make it a good candidate as a medical machine for protontherapy and biological research. Advantages of FFAG for cancer treatment are discussed. Particle tracking tools developed are presented. Machine design constraints and the spiral magnet design undertaken in the frame of the RACCAM project are described. Finally, a comparison of beam dynamic results from spiral FFAG field models in Zgoubi tracking code and from TOSCA 3D models is presented.

## I. INTRODUCTION

Fixed Field Alternating Gradient (FFAG) accelerators are under study all around the world for many applications such as muon acceleration<sup>1</sup> and high intensity proton beam acceleration<sup>2</sup> in neutrino factory schemes, for accelerator driven system (ADS) in subcritical reactor research<sup>3</sup>, and for medical applications: Boron Neutron Capture Therapy (BNCT)<sup>4</sup>, hadrontherapy with protons or light ions<sup>5</sup>.

The RACCAM project<sup>6, 7</sup>, a French ANR supported project, is deeply involved into FFAG research as its goals are:

- To constitute in France a team of accelerator physicists / engineers active in FFAG, beam dynamics and 3D magnet calculations.
- To contribute to theoretical studies and to on-going international FFAG R&D activities.
- To study the use of proton FFAGS in the medical domain, in view of the radiological treatment of tumours.

We focused on a so-called "scaling" type FFAG with spiral magnetic edges for a possible protontherapy machine design from which we will build a magnet prototype.

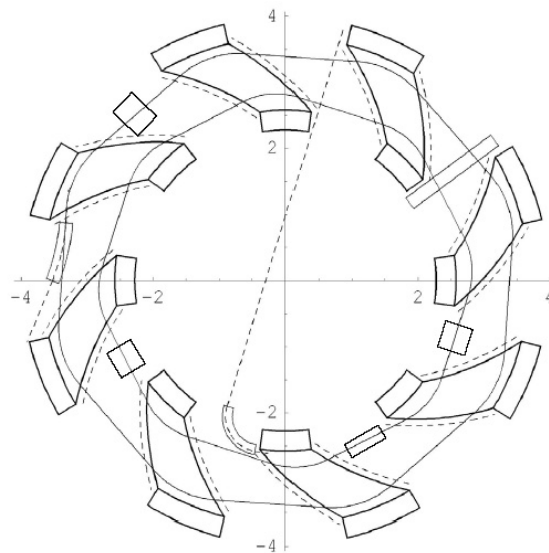


Figure 1: Layout of spiral FFAG for protontherapy. Note the compact size of the ring (dimensions in m).

## II. PROPERTIES OF FFAG FOR MEDICAL APPLICATIONS

Here we give main properties of FFAG accelerators, which motivate an interest in using them as a medical machine:

- High repetition rate, for bunch to pixel scanning with high dose delivery.
- Variable extraction energy.<sup>8</sup>
- Simple and efficient extraction, which results in low machine activation.
- Compact size compared to synchrotrons and cost close to cyclotrons.
- Easy and stable operation due to constant magnetic field during acceleration.

### III. TRACKING CODE DEVELOPMENTS

To simulate particle trajectories and determine beam dynamic parameters in spiral FFAG rings, a Fortran routine - called FFAGSPI - modeling the magnetic field and derivatives (on and off median plane) of a spiral FFAG magnet has been created in the step-by-step trajectory integration code Zgoubi<sup>9,10</sup>.

The field law in the median plane is the following<sup>11</sup>:

$$B = B_0 \left( \frac{R}{R_0} \right)^k F(R, \theta) \quad (\text{Eq.1})$$

where  $B_0$ ,  $R_0$  are reference magnetic field and radius for calculations,  $k$  is the magnetic field index.

$\left( \frac{R}{R_0} \right)^k$  describes the radial behavior of the magnetic field while  $F(R, \theta)$  describes the azimuthal shape of  $B$ , especially in the fringing field region (see Fig. 2).

$F(R, \theta)$  is computed using Enge fringing field models<sup>12</sup> and a fringing field extent  $\lambda$  which was assimilated to the magnetic gap height at first. For a "gap shaping" magnet where the gap is decreasing with the orbit radius (see Part V),  $\lambda$  had to decrease with radius and had a reference value at extraction radius of 40 mm. But now,  $\lambda$  value with respect to the orbit radius is chosen by fitting beam dynamic results from TOSCA 3D models (see Part. VI).

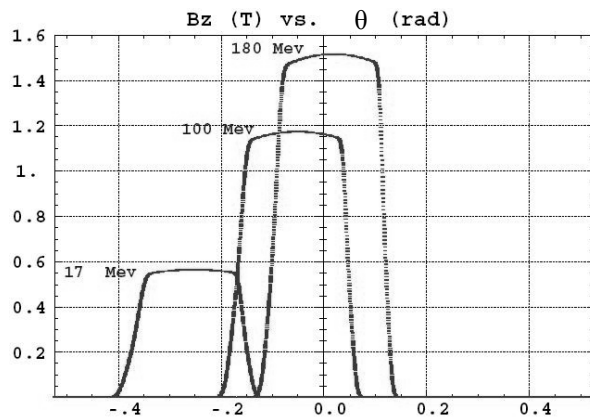


Figure 2: Spiral FFAG magnetic field modeled in Zgoubi code for 17, 100 and 180 MeV proton kinetic energies.

From there, automatic dynamic parameter search (closed orbits, tunes and dynamic acceptances at any energy) have been developed using Zgoubi code.<sup>13</sup>

Moreover, an automatic scanning procedure of magnet parameters ( $k$ ,  $\xi$ ),  $\xi$  being the spiral edge angle with a radius of the ring, has been created<sup>14</sup>. It allows the study of many possible working points ( $Q_x$ ,  $Q_z$ ) in the tune

diagram as  $Q_x$  varies as  $\sqrt{1+k}$  and  $Q_z$  as  $\sqrt{-k + f(1 + 2 \tan^2(\xi))}$ ,  $f$  being the magnetic flutter<sup>11</sup>.

Thanks to the automatic parameter procedure described above, tunes and dynamic acceptances (DA) (horizontal and vertical) can be computed for every ( $k$ ,  $\xi$ ). Fig. 3 illustrates this procedure where magnet parameters are those in Table 1 except for ( $k$ ,  $\xi$ ) varying. Such graphics are used to choose appropriate working points for TOSCA 3D modeling (see Part. V and VI).

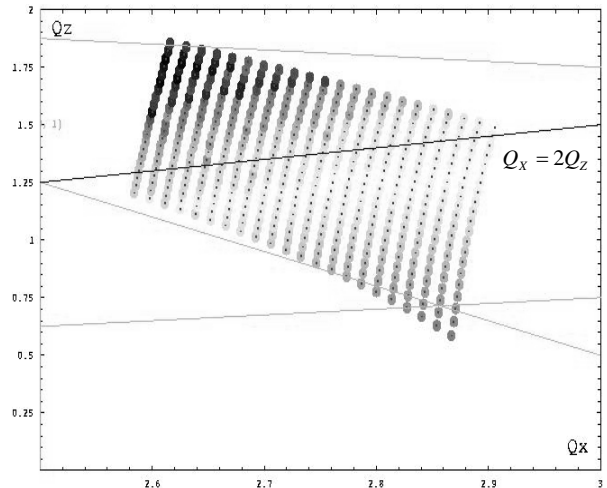


Figure 3: Horizontal dynamical acceptance scan in the tune diagram. Points with larger DA are marked with darker points. Sextupolar resonance  $Q_x = 2Q_z$  is indicated.

### IV. SPIRAL FFAG RING DESIGN CONSTRAINTS

The design of the medical machine for protontherapy within the RACCAM project is based on the following constraints:

Spiral scaling type of FFAG accelerator was chosen due to compact size and zero chromaticity condition, which avoids resonance neighboring during acceleration assuming single RF cavity with voltage of about 5 -10 kV.

A relatively small number of lattice cells of 8 or 10 was assumed in order to avoid fringing field dominated magnet design. On the other hand small number of lattice cells does not allow large field index values, which dictates rather large orbit excursion and increases the magnet weight and cost. The cell number of 10 is a compromise between the minimization of the magnet weight and the need for straight section length mainly for cavity placement and injection/extraction systems.

Both injection and extraction are based on horizontal phase space because of relatively predictable behavior of the horizontal focusing and dynamical acceptance in

contrast to the vertical plane. In addition the need for multiturn injection in order to store beam intensity up to a few  $10^9$  protons dictates the horizontal fractional tune to be around 0.2 or 0.8 in order to enable horizontal betatron stacking with typical 50 % efficiency in about 10 turns. Additional possibility of the combined horizontal-vertical stacking would result in similar constraint in the vertical plane.

The issue of space for RF cavity placement between spiral magnet boundaries dictates small magnet packing factor and spiral angle as small as possible. In addition the fact that the closed orbit through the RF cavity is not always parallel to the accelerating electric field introduces synchrotron coupling. In order to minimize its effect on the beam emittance during RF capture and acceleration it is preferable to place RF cavity perpendicular to the injection orbit, which makes the problem of room in the straight section even more difficult.

In order to be below the iron saturation limit, what is required by the variable energy operation scheme, the magnetic field seen by the beam was chosen not to exceed 1.5 T on the median plane. Recent estimations suggest that this value may be increased up to 1.7 T.

Table 1: Parameters of spiral FFAG ring described.

Number of cells	8
Injection energy range	6-17 MeV (AIMA cyclotron)
Corresponding extraction energy range	70-180 MeV
Injection type	multiturn by betatron stacking
Extraction type	fast with kicker
Magnetic field index k	4.415
Spiral angle $\xi$	$50.36^\circ$
Fringing field extent $\lambda$	83 mm
Packing factor	0.34
$B_{\max}$	1.5 T
$R_{\max}$ (extraction)	3.5 m
$R_{\min}$ (injection)	2.9 m
Gap height (injection)	92 mm
Gap height (extraction)	40 mm
Harmonic number	1
Hor. / Vert. tunes ( $Q_x, Q_z$ )	(2.80, 1.34)

Working point should be located well outside of the systematic resonances and characterized by good dynamic acceptances in both transverse planes.

Extraction energies between 70 – 180 MeV (180 MeV corresponding to 21cm penetration depth in water<sup>15</sup>) was chosen as a compromise between the medical needs and injection/extraction momentum ratio of 3.4. The corresponding injection energy range is 6-17 MeV.

Layout of the example design of a spiral FFAG ring is shown in Fig. 1 and its several parameters are listed in Table 1. This example is not taken as a final design for a machine because tunes are too close from systematic sextupolar resonance  $Q_x=2Q_z$  (see Figure 3). This set of parameters is presented to show typical results and comparisons between FFAGSPI and TOSCA 3D models (see Part VI).

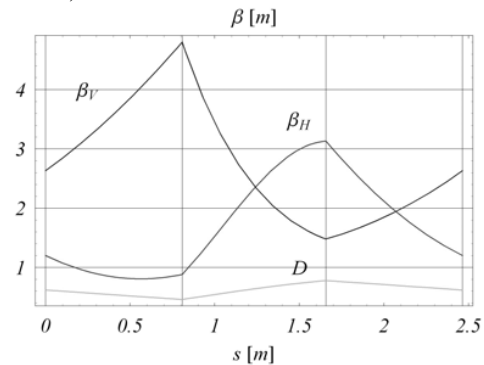


Figure 4: Horizontal and vertical betatron ( $\beta_H, \beta_V$ ) and dispersion (D) functions in one cell of the spiral FFAG ring.

Fig. 4 shows betatron function and dispersion in one lattice cell computed with Mathematica / BeamOptics<sup>16</sup>. The alternating focusing at the entrance and the exit magnet edges is clearly seen.

## V. MAGNET DESIGN

Two types of magnet design were considered for the spiral FFAG ring:

- Based on usual "gap shaping" technology (see Fig. 5 and 6). This type shows up initially the largest vertical tune excursion. Recent results with chamfer variable with radius and field clamps produced almost constant vertical tune as a function of energy.<sup>17</sup> (see Fig. 7 and 8)

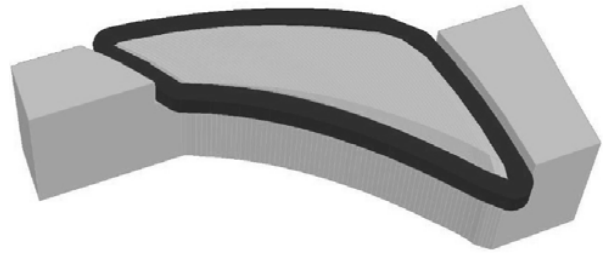


Figure 5: 3D view of the "gap shaping" magnet. The magnetic field is produced by a single coil.

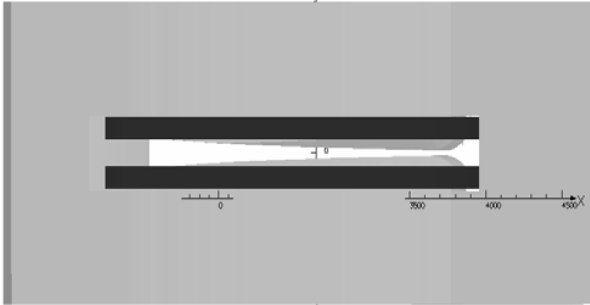


Figure 6: Side view of the "gap shaping" magnet. The gap height varying with radius can be seen.

- "Parallel gap with distributed conductors", where the scaling field law (Eq. 1) is produced by independently powered series of conductors distributed on magnet poles<sup>18</sup>. In spite of smaller tune excursion due to parallel gap assumption this type is liable to produce large field under/overshoots depending on the distributed current intensities. Research continues to investigate this method.

## VI. COMPARISON FFAGSPI / TOSCA 3D MODELS

Development of FFAGSPI routine modeling a spiral FFAG magnetic field is to have a powerful tool to simulate particle trajectories in such a magnet. We want our model to give beam dynamic results as close as a TOSCA 3D model. In that case, we can predict particle dynamics in a spiral FFAG magnet roughly in a half-hour using the FFAGSPI routine while it takes several days to build a TOSCA 3D model. The goal is to make our tool extremely powerful to study many working points to find the best set of parameters for TOSCA 3D modeling, then for magnet prototyping and finally for a protontherapy FFAG accelerator.

Our approach is the following. Several hundreds working points have been studied using the numerical tools developed and presented in Part III. Tunes and dynamic acceptances have been calculated using Zgoubi code and its FFAGSPI routine to finally choose a set of parameters for model comparisons (see Table 1). From there, a TOSCA 3D model has been built and tracking was done using a 2D field map constructed from the 3D model. Comparison between beam dynamic results from FFAGSPI and TOSCA is the next step and is illustrated on Fig. 7 and 8.

Figure 7 shows horizontal and vertical tunes with respect to the particle kinetic energy for FFAGSPI simulations with initial fringing field extent  $\lambda$  equal to the gap height ( $\lambda=92$  mm at injection radius and 40 mm at extraction) and for tracking in a 2D field map from TOSCA model. The  $Q_z$  blue curve is the vertical tune behavior we expected for a "gap shaping" magnet without chamfer or clamps. The difference is obvious and can be explained. First, magnet design with variable chamfer and

field clamps reduces the vertical tune shift between 17 MeV and 180 MeV from 0.8 to 0.35 and this is why the red curve is flatter than the blue one. In particular, variable chamfer and field clamps makes the fringing field extent to be constant from injection to extraction radius. The main problem is that we can not predict the result from TOSCA 3D with FFAGSPI model at that step. That means the working point expected for a set of parameter would be totally different once TOSCA models will be constructed.

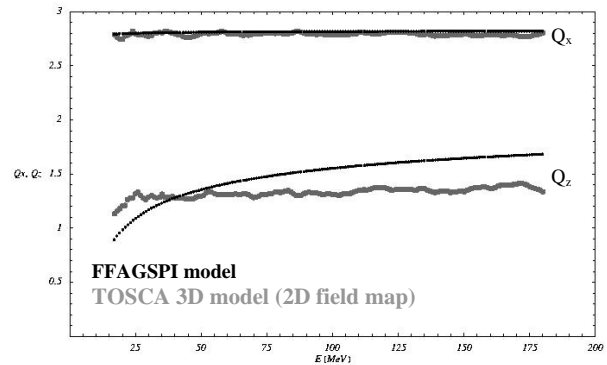


Figure 7: Horizontal ( $Q_x$ ) and Vertical ( $Q_z$ ) tunes for FFAGSPI ( $\lambda \approx$  gap height,  $\lambda$  varies with radius) and TOSCA 3D models.

This is why the next step was to take into account this particular magnet design to fit  $\lambda$  in FFAGSPI model. The goal is to find tunes as in TOSCA 3D model.  $\lambda$  value was found equal to 83 mm and constant from injection to extraction radii, that value is now used in tracking simulations described in Part. III.

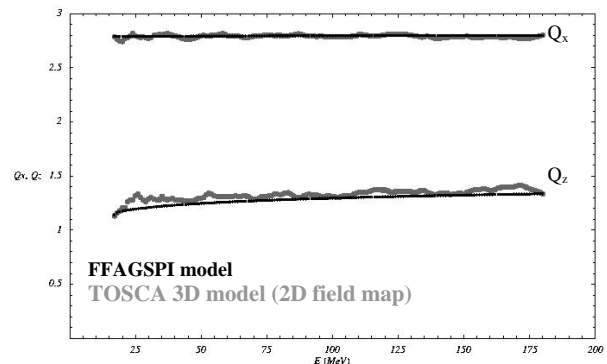


Figure 8: Horizontal and Vertical tunes for FFAGSPI (fitted  $\lambda=83$ mm, constant with radius) and TOSCA 3D models.

This comparison between TOSCA 3D and FFAGSPI with fitted  $\lambda$  is shown on Fig. 8. It is obvious the agreement is better than on Fig. 7. We are confident we can elaborate a better fitting procedure of  $\lambda$  in FFAGSPI and smooth the horizontal and vertical tune oscillations in TOSCA – by improving the model (field integral

precision to  $10^{-4}$  and more accurate magnet edge spiral shape) and the tracking numerical methods.

Fig. 9 shows the horizontal dynamic acceptances at 17, 60, 100, 140 and 180 MeV for FFAGSPI ( $\lambda=83\text{mm}$ ) and TOSCA 3D models. We can see that the agreement is excellent between both models. The shift between red and blue points on Fig. 9 is chosen arbitrarily to facilitate the comparison.

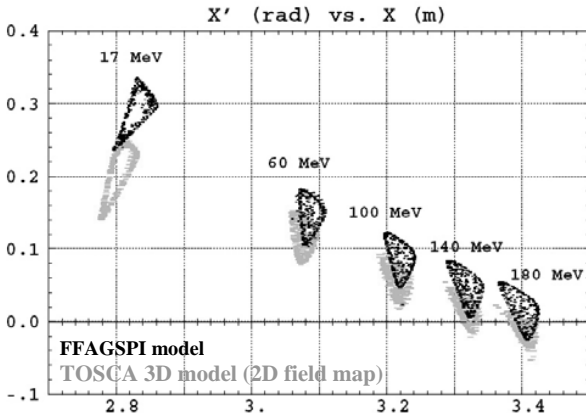


Figure 9: Horizontal acceptances at 5 energies for FFAGSPI (fitted  $\lambda=83\text{mm}$ , constant with radius) and TOSCA 3D models.

The same study has been done for different working points in order to make sure our procedure can be repeated for any set of parameters and the results are the same: beam dynamics is similar from FFAGSPI to TOSCA. FFAGSPI models with fitted  $\lambda$  value is now intensively used to study tunes and dynamic acceptances for many different sets of magnet parameters in order to choose few candidates for TOSCA 3D modeling, magnet prototyping and protontherapy FFAG ring design studies.

Similar beam dynamic comparisons will be undertaken using the same FFAGSPI model with fitted parameters but the 2D field maps will be replaced by a 3D field map constructed from the TOSCA 3D model. In that way, models will be improve again in order to have a powerful and fast numerical simulation tool to design a protontherapy spiral FFAG ring.

## VII. CONCLUSIONS

Substantial progresses have been achieved in tracking code and TOSCA magnetic simulation development tools within the RACCAM ANR project. The excellent beam dynamic result comparisons between FFAGSPI and TOSCA models are very encouraging towards the design of a variable energy spiral scaling FFAG accelerator for protontherapy. The ring parameters have been investigated and the method to design the spiral magnet fulfilling the scaling properties, in particular zero

chromaticity condition have been established. Work will continue towards the magnet prototype construction and hopefully in farther future towards the demonstration machine.

## REFERENCES

1. A feasibility study of a neutrino factory in Japan, KEK Report, February 2001.
2. FFAG Accelerator Proton Driver for Neutrino Factory, A.G. Ruggiero, Proceedings to the 7<sup>th</sup> International Workshop on Neutrino Factories and Superbeams, May 2006, pp 315-317.
3. Construction of FFAG Accelerator in KURRI for ADS Study, Y. Mori et al., Proceedings of EPAC 2004, Lucerne, Switzerland.
4. Study of Compact Medical FFAG Accelerators and their applications for intense secondary particle production, Y. Mori, NIM A 562-2, June 2006, pp 591-595.
5. Study of Compact Medical FFAG Accelerators, T. Misu, FFAG04 Workshop, KEK, Japan.
6. The FFAG R&D and Medical Application Project RACCAM, F. Méot et al., Proceedings of EPAC 2006, Edinburgh, Scotland.
7. <http://www.lpsc.in2p3.fr/RACCAM/>
8. Spiral FFAG for protontherapy, J. Pasternak et al., PAC 2007, Albuquerque, USA.
9. Zgoubi User's guide (v4.3), F. Méot, S. Valero, Rapport DAPNIA-02-395, 2003.
10. Developments in the ray-tracing code Zgoubi for multiturn tracking in FFAG rings, F. Lemuet, F. Méot, NIM A 547, 2005, pp 638-651.
11. Spiral sector magnets, D. W. Kerst, MURA-112, 1956.
12. Deflecting magnets, H. A. Enge, in *Focusing of charged particles*, Vol. 2, A. Septier ed., Academic Press, New-York and London (1967).
13. Développements de codes de simulations de FFAG spiral et de programmes d'automatisation de balayage de paramètres, J. Fourier, LPSC 04-47 Internal Report, 2007.
14. Spiral FFAG lattice design tools. Application to 6-D tracking, F. Méot et al., LPSC Internal Report submitted to NIM, May 2007.
15. Simulation du dépôt d'énergie du faisceau de proton du FFAG dans l'eau, A. Chaikh, LPSC Internal Report, 2007.
16. BeamOptics, a program for analytical beam optics, B. Autin et al., CERN Yellow Report 98-06, 1998.
17. 3-D Magnetic calculation methods for spiral scaling FFAG Magnet Design, T. Planche et al., PAC 2007, Albuquerque, USA.
18. Magnet Simulations for Medical FFAG, B. Autin, E. Froidefond, Proceedings of EPAC 2006, Edinburgh, Scotland.